Stability of Highly OH-Covered C_{60} Fullerenes: Role of Coadsorbed O Impurities and of the Charge State of the Cage in the Formation of Carbon-Opened Structures

J. G. Rodríguez-Zavala

Departamento de Ciencias Exactas y Tecnológicas, Centro Universitario de Los Lagos, Universidad de Guadalajara, Enrique Díaz de León S/N, 47460 Jalisco, México

R. A. Guirado-López*

Instituto de Física "Manuel Sandoval Vallarta", Universidad Autónoma de San Luis Potosí, Alvaro Obregón 64, 78000 San Luis Potosí, México

Received: March 24, 2006; In Final Form: June 2, 2006

We have performed both semiempirical as well as ab initio density functional theory calculations in order to investigate the structural stability of highly hydroxylated $C_{60}(OH)_{32}$ fullerenes, so-called fullerenols. Interestingly, we have found that low-energy atomic configurations are obtained when the OH groups are covering the C_{60} in the form of small hydroxyl islands. The previous formation of OH molecular domains on the carbon surface, stabilized by hydrogen bonds between neighboring OH groups, defines the existence of $C_{60}(OH)_{32}$ fullerene structures with some elongated C−C bonds, closed electronic shells, and large highest occupied−lowest unoccupied molecular orbital energy gaps, with the latter two being well-known indicators of high chemical stability in these kind of carbon compounds. The calculated optical absorption spectra show that the location of the first single dipole-allowed excitation strongly depends on the precise distribution of the OH groups on the surface, a result that, combined with optical spectroscopy experiments, might provide an efficient way to identify the structure of these kinds of fullerene derivatives. We found that the presence of a few coadsorbed oxygen species on the fullerene surface leads in general to the existence of $C_{60}(OH)_{32}O_x$ ($x = 1-4$) compounds in which some of the C−C bonds just below the O impurities are replaced by C−O−C bridge bonds, leading to the formation of stable carbon-opened structures in agreement with the recent experimental work of Xing et al. (*J. Phys. Chem. B* **2004**, *108*, 11473). Actually, a more dramatic cage destruction is obtained when considering multiply charged $C_{60}(OH)_{32}O_x^{\pm m}$ ($m = 2, 4, 6$) species (that can exist in both gas-phase and aqueous environments), where now sizable holes made of 9- and 10-membered rings can exist in the carbon network. We believe that our results are important if the controlled opening of carbon cages is needed and it should be taken into account also in several technological applications where the permanent encapsulation of atomic or molecular species in these types of fullerene derivatives is required.

I. Introduction

The design of new materials with novel and special properties is presently the subject of intense investigation. In particular, fullerene related materials have attracted a lot of attention, since, besides the fact that they can be produced in large quantities with full control over size and morphology, they have also demonstrated that they possess a lot of interesting properties that could lead to the development of novel technologies. As is well-known, C_{60}, a hydrophobic molecule made of 60 carbon atoms arranged in a soccer ball shape,[1] is the backbone of the fullerene-based nanomaterial family. In fact, the structural, electronic, and solid-state properties of this molecule have attracted wide interest not only in physics and chemistry but also in materials and biological sciences.

As part of the remarkable progress made in this field, in the last years, it has been demonstrated that the behavior and processing of the C_{60} fullerene can be strongly modified via the chemical functionalization of its surface, that is, by covalently attaching several types of atoms, molecules, or molecular groups.[2−4] The previous finding has led to the fabrication of a large number of organic derivatives and has significantly expanded the scope of the science of these kinds of carbon clusters. In particular, several types of functionalized C_{60} molecules have been recently synthesized for their possible use in new electronic and optical devices as well as for developing possible applications in biology and medicine. For example, the use of functionalized fullerenes as photoactive molecular systems has been recently discussed, being particularly important for the conversion of solar energy into electric current.[5] In addition, C_{60} derivatives have been proposed to be HIV protease inhibitors[6] and to promote interactions with target molecules,[6−8] such as a particular protein on a cell surface. They have been defined also as potent antioxidants[9] and as neuroprotectants in vivo[10] and finally, if metal atoms can be trapped in the inside of the carbon cage, as good candidates for a new generation of novel magnetic resonance imaging (MRI) contrast agents.[11]

At this point, it is important to mention that a large amount of the fullerene research mentioned in the last paragraph has involved the use of highly hydroxylated $C_{60}(OH)_x$ compounds (fullerenols).[12] These water-soluble fullerene derivatives can be

* To whom correspondence should be addressed. E-mail: guirado@ifisica.uaslp.mx.

10.1021/jp061855m CCC: $33.50
Published on Web 07/12/2006

synthesized by means of several experimental techniques, as clearly reviewed in ref 13, and their properties have been extensively analyzed in both gas-phase and aqueous environments, as well as in the form of deposited nanostructures, by means of infrared spectroscopy (IR),[14] transmission electron microscopy (TEM) images,[4] dynamic light scattering (DLS) measurements,[15] X-ray photoelectron spectroscopy (XPS),[13,14] and optical absorption experiments,[5] among others. The previous experimental characterization has revealed important information concerning the average number of adsorbed OH groups on the carbon surface and its impact on the partial or total solubility of the carbon compound, the presence and role of impurities in the samples, their intermolecular interactions and aggregation behavior, the electrical conductivity, and the optical properties in both ultraviolet and visible parts of the spectra.

However, despite the already mentioned extensive characterization, there are of course additional points of interest that need to be addressed, among which the most important are the ones related to the study of the structural stability of these highly hydroxylated C_{60} fullerenes in different environments. It is clear that the inclusion of these fullerene derivatives in gaseous, aqueous, or solid-state matrixes might alter their chemical composition as well as the charge state of the cage, a fact that could lead to the formation of carbon-opened structures, strongly affecting thus their properties and functionality. Furthermore, understanding the precise microstructural features and fundamental physics leading to the cage destruction of these nanometer-sized carbon structures will be of fundamental importance in order to attain the controlled ring opening (and closing) of the carbon cage,[16] which is also relevant to allow the inclusion of different types of guest species that are not accessible by conventional methods, such as those based on coevaporation techniques[17] or high-pressure/high-temperature experiments.[18]

In this respect, recently Xing et al.[14] have reported an extensive experimental investigation in order to analyze the structural stability of highly hydroxylated $C_{60}(OH)_x$ ($x = 30$, 32, 36, 42, 44) fullerenes as a function of the degree of surface coverage and impurity content. These authors have found, by using the laser-induced dissociation technique, that the molecular stability is not very sensitive to the number of OH groups adsorbed on the C_{60} but critically depends on the concentration and type of impurities coadsorbed on the fullerene surface. In particular, the presence of oxygen atoms was found to be the key factor leading to the formation of cage-opened structures, a result that underlines, for the first time, the importance of producing high-purity fullerene derivatives in order to obtain stable closed-cage carbon networks. In agreement with the previous experimental data, Husebo et al.[13] also found that their synthesized fullerenol compounds were not simply polyhydroxylated C_{60} but instead a more complex fullerene structure containing also chemisorbed oxygen atoms that naturally appear in the reaction and that it seems that they cannot be turned away from the formation process. In addition, they have revealed that these kinds of fullerene derivatives actually exist as stable, multiply charged anions, a result that is consistent with the well-known ability of the C_{60} molecule to retain an excess of electronic charge.[19] Unfortunately, the authors of ref 13 did not discuss if their synthesized fullerene derivatives were able to exist as stable closed- or open-cage configurations.

At this point, we must comment that, even if in both experimental setups it was possible to estimate the average number of adsorbed OH's on the C_{60} and identify the chemical nature of all the species attached to the carbon structure, it is also clear that most of the research involving polyhydroxylated fullerenes has been carried out without a detailed understanding of the structural organization of the OH groups on the surface of such small objects. Obviously, the precise location of the adsorbates on these kinds of spheroidal carbon networks is at the origin of the reported structural stability and of the observed physical and chemical properties over a large scale. It is thus of fundamental importance to provide additional information about the atomic structure that goes beyond the current experimental evidence, and in consequence, we have decided to present in this work a systematic theoretical investigation dedicated to analyze the structural stability of neutral and ionized highly hydroxylated $C_{60}(OH)_{32}$ fullerenes in order to shed some more light onto the understanding of the measured data.

Here, we systematically study, by using both semiempirical (PM3) and density functional theory (DFT) approaches, the influence of the number, type, and spatial distribution of the adsorbates in the carbon surface on the energetics and electronic and optical properties of highly OH-covered structures. We found that the OH groups seem to prefer to cover the C_{60} surface in the form of small hydroxyl islands stabilized by the existence of hydrogen bonds between neighboring OH groups. We find that the optical gap of each one of our considered fullerenols differs in position as well as in the intensity of the excitation, a fact that we believe is enough to distinguish all of our considered isomers. Finally, we define the approximated critical concentration (and location) of oxygen impurities as well as the amount of extra (or missing) electronic charge required to obtain the rupture of the cage. We conclude that the understanding of the experimental measurements on functionalized C_{60} structures should consider more subtle effects related to the chemical composition, the charge state of the cage, and the precise disposition of the adsorbates on the carbon surface.

The rest of the paper is organized as follows. In section II, we briefly describe the theoretical models used for the calculations. In section III, we present our results analyzing the structural aspects and electronic behavior, and finally, in section IV, the summary and conclusions are given.

II. Theoretical Modeling

To better understand the experimental data reported in refs 13 and 14, we will perform a systematic theoretical study of the structural, electronic, and optical properties of various gas-phase-like $C_{60}(OH)_{32}$ structures. We will consider several configurations for the adsorbed OH groups on the C_{60} surface, and even if this procedure does not necessarily lead to the global minimum, nonetheless, it will provide stable low-energy configurations which are best viewed as representative structures which is all that is required in the present study.

We will try to understand the reported structural stability by analyzing the contribution of the number and type of adsorbates (OH groups as well as some oxygen impurities) present in the system as well as the type of adsorbed molecular phases stabilized on the C_{60} surface. The number of atoms involved in our considered systems (up to ~125 atoms) limits the applicability of accurate density functional theory (DFT) optimization-based methods, and that is why we have decided to perform our systematic study by combining different theoretical approaches. In a first step, we have fully optimized our considered $C_{60}(OH)_{32}$ structures using the PM3 Hamiltonian[20] which is well-known to provide a very good description of hydrogen-bond-containing systems, and then, in a second step, we have used these PM3 molecular geometries to perform single-point density functional theory (DFT) calculations in order to more accurately obtain the electronic structure and the relative stability

between the different considered isomers. In particular, the Kohn−Sham equations are solved by using the hybrid B3LYP expression[21] for the exchange-correlation potential together with the 6-21G basis set,[22] which is a good compromise between computational cost and accuracy.

Finally, we will also use the previously obtained PM3 molecular geometries to simulate the absorption spectra of our fullerenol compounds by calculating their excitation energies, the corresponding oscillator strengths, and the optical gap (defined as the first single dipole-allowed excitation) within the framework of the semiempirical Zerner intermediate neglect of diatomic differential overlap (ZINDO) method.[23] These calculations are interesting to perform, since the comparison of theoretical data with (if available) optical spectroscopy experiments has already been defined as an efficient tool to identify the possible structure of fullerene derivatives. All three methods—PM3, ZINDO, and DFT—were used as implemented in the Gaussian 98 software.[24] Our hybrid procedure could be justified, since the accuracy of both the semiempirical PM3 and ZINDO methods has been proven in several calculations addressing the structural and optical properties of fullerene materials. In particular, the ZINDO Hamiltonian has been successfully applied to the calculation of the absorption spectra of a large number of fullerene derivatives (see ref 3 and references therein). Within this methodology, the self-consistent field calculation is followed by a configuration interaction calculation in which only single excited configurations are taken into account. We have included a maximum of 6400 excited configurations in all of our calculations which corresponds to all single excitations from the 80 highest occupied to the 80 lowest unoccupied molecular orbitals, which is large enough to ensure that the energies and intensities of the lowest excited states become essentially stable even if we still increase our configuration space. The resulting data, which constitute a bar spectrum, can be compared with the data obtained from optical absorption experiments.

The numerical accuracy of our hybrid methodology is tested by calculating the well-known structural and optical properties of the C_{60} molecule. For the C_{60} fullerene, the PM3 method finds C−C bond lengths of 1.457 and 1.383 Å for single and double bonds, respectively, in good agreement with gas-phase electron studies (1.458 ± 0.006 and 1.401 ± 0.010 Å)[25] and more elaborated calculations (1.446 and 1.406 Å).[26] On the other hand, focusing on the experimentally measured low-energy excitations (below 4.5 eV) for fullerenes in the gas phase[27] or solution,[28] it is well-known that there are only two dipole-allowed transitions around 3.05 and 3.8 eV. The ZINDO method nicely reproduces these values, since our calculated first and second allowed excitations for the C_{60} molecule are located at 3.19 (∼388 nm) and 3.83 eV (∼323 nm), having oscillator strengths of 0.003 and 0.67, respectively. Finally, the ZINDO method finds that the first singlet excitation of the absorption spectra, which is in fact optically forbidden, is located at 2.27 eV (∼544 nm), a value that is in good agreement with the ones found with more sophisticated theoretical approaches, such as those involving the use of time-dependent density functional theory (TD-DFT), which report values in the range 2.1−2.3 eV (see Table 1 of ref 29).

It is important to establish also the accuracy of our hybrid methodology in describing the interacting OH + C_{60} system. From our PM3 calculations, we have found that the adsorption of a single OH group on the C_{60} surface results in a chemisorbed configuration in which the hydroxyl group is directly adsorbed (through the O atom) on top of a C atom of the cage, having C−O and O−H bond lengths of 1.40 and 0.95 Å, respectively, and a C−O−H angle of 106.3°. It is interesting to compare the previous structural parameters with the ones obtained using more sophisticated methodologies. Consequently, we have decided to perform additional test calculations for the $C_{60}OH$ system in which we fully optimize our single hydroxylated C_{60} molecule within the DFT framework, using the hybrid functional B3LYP[21] and the 6-21G basis set. From these calculations, we have found C−O and O−H bond lengths of 1.46 and 1.0 Å together with a C−O−H angle of 106.3°. As expected, notice that the semiempirical approach slightly underestimates the bond lengths (by ∼5%) when compared with the DFT data; however, we note that the C−O−H tilting angle is correctly reproduced. As a consequence, it is thus necessary to quantify how these structural differences affect the quality of our calculated (single-point) total energies, which determine the relative stability between our considered isomers.

To qualitatively discuss the previous effects, we have performed additional calculations on the well-known $C_{60}(OH)_2$ compound, the so-called fullerene diol. We consider two contrasting atomic configurations in which the OH groups are located in opposite sides of C_{60} and adsorbed on adjacent C atoms (forming a double bond) of the cage. Our combined PM3/DFT methodology reveals that the later atomic array is more stable than the former by 2.04 eV. This result is in agreement with the report of Meier and Kiegiel[30] who have experimentally identified the existence of this type of adsorbed configuration. On the other hand, by fully optimizing our fullerene diols within the B3LYP/6-21G approach, we obtain the same energy ordering with a very similar energy difference of 2.18 eV. From this set of calculations, it is clear that the correct relative stability is predicted by our hybrid methodology.

Finally, we analyze also the single OH adsorption on a (10,0) carbon nanotube, to compare further our semiempirical structural data but now with recent DFT pseudopotential studies reported by Pan et al.[31] performed on the same system. From the PM3 calculations, we found that the OH group is adsorbed, through the O atom, on top of a C atom of the tube, the C−O and O−H bond lengths are equal to 1.42 and 0.95 Å, respectively, and a C−O−H angle of 106.2° is obtained. The C−C distances around the adsorption site are slightly perturbed, having values in the range 1.50−1.53 Å, and the three C−C−O angles around the OH group vary from 105.7 to 111.25°. These values are in reasonable agreement when compared to the ones found in the ab initio pseudopotential calculations of ref 31 where the on-top chemisorbed configuration has also been found to be the most stable, having values of $R_{C-O} = 1.48$ Å and a C−O−H angle of ∼100°. In addition, the angles between the O−C bond and C−C bonds around the adsorption site fall in the range 107−112°, and the C−C bond lengths just below the OH molecule are within 1.52 Å. As we can see, the agreement between our methodology and the experimental measurements as well as more elaborated calculations is very satisfactory and serves as a basis to discuss the structural, electronic, and optical properties of our considered highly hydroxylated fullerenes.

III. Results and Discussion

Of course, without experimental guidance as to the isomer that is actually produced, it is prohibitively time-consuming to categorize the many possibilities in which the OH groups can be adsorbed on the C_{60} surface. Here, our structural search for the lowest energy $C_{60}(OH)_{32}$ structure is based on various initial configurations in which, following previous experimental[5] and theoretical[32] work, we consider 32 OH groups (1) homoge-

neously distributed on the surface, (2) aggregated on one side of the C_{60} cage, and (3) forming various $(OH)_n$ hydroxyl islands of different sizes and with varying spatial distributions. As previously stated, we do not attempt to perform an extensive exploration of all of the resulting $C_{60}(OH)_{32}$ isomers but instead attempt to compare with previous theoretical works and to try to reveal more general tendencies concerning the possible adsorbed configurations that can be adopted by the OH groups on the C_{60} surface as well as their influence on the structural stability, electronic, and optical properties of these highly hydroxylated carbon compounds.

In Figure 1, we show the calculated PM3 lowest energy atomic arrays for our considered $C_{60}(OH)_{32}$ initial configurations mentioned above. In all cases, the OH molecules have been found to be directly adsorbed on top of a carbon atom of the fullerene cage having average values for the C−O and O−H bond lengths of 1.4 and 0.95 Å, respectively. In all of our optimized structures, the OH molecules are tilted away from the surface normal with average C−O−H angles that fall in the range 105−110°. However, even if our results indicate that the OH groups are not adsorbed with a preferred C−O−H angle, we note that in some of the adsorbed phases (mainly in those shown in Figure 1a−c) the relative orientation between neighboring OH molecules is strongly correlated, since the positively charged H atoms are mostly pointing toward their nearest negatively charged O species, forming a weakly connected (hydrogen-bonded) molecular layer. Interestingly, the existence of a similar microscopic effect has been used to explain the stability of highly hydroxylated Pt surfaces[33] where the presence of hydrogen-bonded hexagonal arrangements of OH groups has been proposed. Finally, from the figure, it is clear that the oxygen−carbon interaction is very strong, since all isomers appear as highly distorted fullerenes and, in addition, some of them are characterized by having various elongated C−C bonds with values as large as 1.7 Å. This result clearly demonstrates the considerable strain and flexibility that can be supported by the C_{60} fullerene and, together with our previous study addressing the low-hydroxylated regime,[32] supports also the experimental observation of Xing et al.[14] that the structural stability of highly hydroxylated C_{60} is not so sensitive to the number of attached OH groups.

As a second step, for all the previously optimized PM3 molecular structures shown in Figure 1, we have performed single-point DFT calculations by using the hybrid B3LYP exchange-correlation functional and the 6-21G basis set, in order to obtain the relative stability and the electronic spectra of all of our considered $C_{60}(OH)_{32}$ isomers. Interestingly, and following our previous work[32] where we found that, in the low-coverage regime (up to 14 adsorbed OH groups), the hydroxyl molecules prefer to organize in small molecular islands on the C_{60} surface, we have surprisingly obtained in the present case the apparent continuation of this kind of growth sequence, since low-energy atomic configurations are always found when the 32 OH groups segregate on the C_{60} surface, forming well-defined molecular domains like the ones shown in Figure 1a and b. Actually, these two configurations are separated by a total energy difference of 0.58 eV, while the rest of the considered isomers are ∼3.3−27 eV less stable (when compared to the fullerenol structure shown in Figure 1a), as shown in Table 1. Interestingly, it is clearly seen that if larger hydroxylated regions are formed on the surface, as shown in Figure 1c, e, and f, or the island formation is suppressed, as shown in Figure 1d and g, the total energy of the system is reduced, defining thus the existence of a well-defined type of adsorbed phase. Notice that, despite the considered high degree of surface coverage, our low-energy atomic configurations are characterized by the existence of still appreciable unprotected carbon regions. However, we believe that the close proximity of the various hydroxylated domains is expected to prevent, by means of the steric repulsions, the incorporation of additional species that could chemically attact the fullerene compound, leading thus to the existence of a very stable carbon derivative.

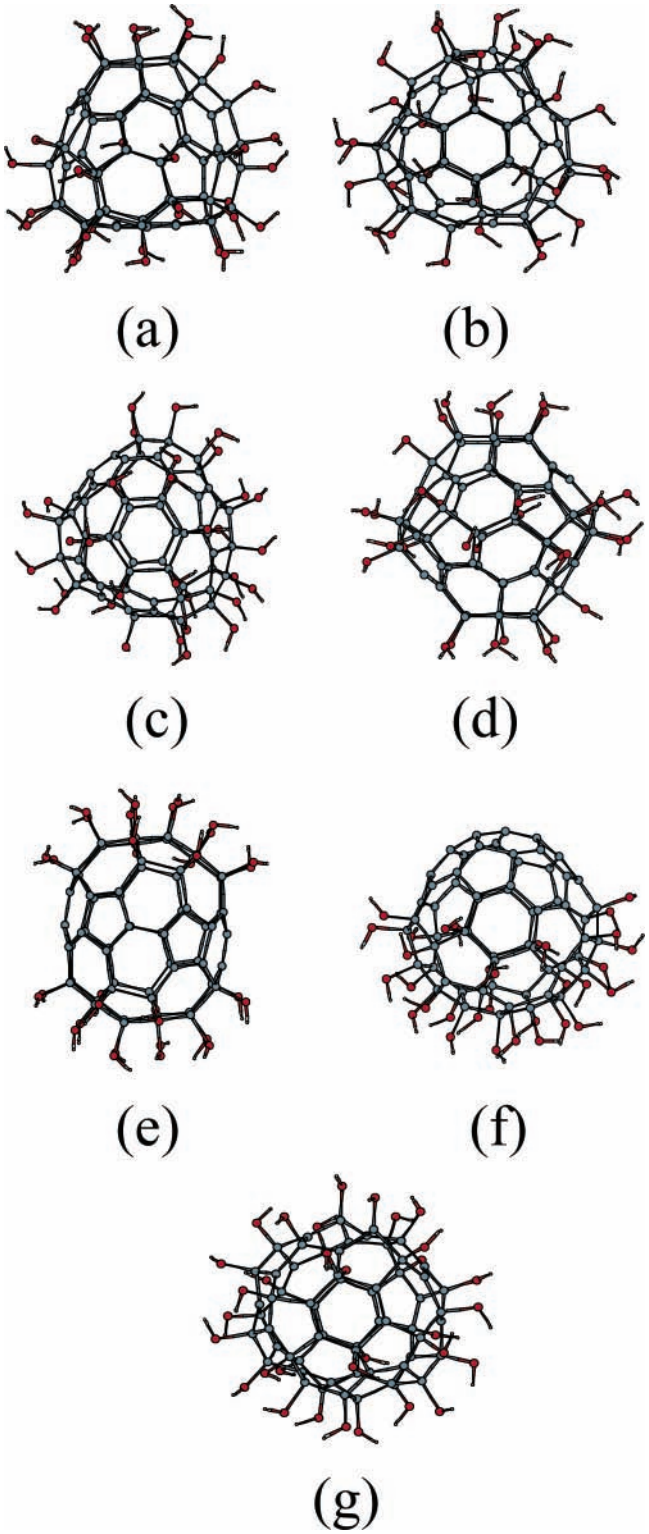

Figure 1. Optimized PM3 atomic configurations for various $C_{60}OH_{32}$ isomers.

TABLE 1: Relative Stability between the Different Considered Isomers Shown in Figure 1

relative stability	ΔE (eV)
1a−1a	0.00
1a−1b	0.58
1a−1c	3.33
1a−1d	3.55
1a−1e	12.87
1a−1f	16.23
1a−1g	27.32

Actually, a similar patchy behavior for the adsorption of H and Cl atoms on the C_{60} surface has been suggested by Fowler et al.[34] and Birkett and co-workers,[35] respectively, and also when small amounts of OH groups are attached to the fullerene surface in the reports of Slanina et al.[36] and Wang and Chong.[37] In addition, it is important to comment that recent time-of-flight mass spectrometry and photoelectron spectroscopy experiments by Palpant et al.[38] have provided evidence of a similar clustering on the C_{60} surface but where Au atoms preferably form a Au_N cluster (for $N = 0-6$) rather than a layered structure spread over the carbon cage. Furthermore, Dugourd et al.[39] have measured the electric polarizability of $C_{60}Na_n$ clusters in the range $1 \leq n \leq 34$ and have concluded that their experimental data are consistent with the formation of a sodium droplet on the surface of the fullerene, an atomic configuration that has been later confirmed by the theoretical calculations of Roques and co-workers.[40] Finally, Sun et al.[41] have recently theoretically found that Ti atoms prefer to cluster also on the C_{60}. In this respect, it is important to mention that, even if the chemical nature and the bonding features of the adsorbates mentioned above (OH groups as well as Au, Na, H, Cl, and Ti atoms) are completely different, it is evident that a patchy behavior on the C_{60} surface can be observed for different atomic as well as molecular species.

Of course, the precise structural details of the adsorbed phases shown in Figure 1 are determined by the distribution of the oxygen−carbon bonds as well as by the noncovalent lateral interactions among the OH groups. The first ones are responsible for producing sizable outward, inward, as well as lateral displacements of the C atoms of the cage, leading to the formation of highly distorted structures. In addition, they also induce notable perturbations all along the electronic spectra (through a notable C → O charge transfer) consisting of sizable changes in the ordering of the eigenvalues, splitting of many of the energy levels that are degenerated in the bare C_{60}, and various HOMO−LUMO gap reopenings and closings. The second ones of course impose a secondary level of organization in which the relative orientation of the OH groups at the end of the optimization cycle will be the ones that minimize the lateral intermolecular interactions, defining thus also the self-organization and packing of the adsorbates on the surface.

In particular, the precise details of the electronic structure and the C−O−H average orientation in each one of the fullerene compounds shown in Figure 1 have been found to play a major role in the calculated energy ordering. First, we have found that there is a strong correlation between the calculated relative stability of the considered isomers and the corresponding energy gap between the highest occupied and lowest unoccupied molecular orbitals. As is well-known, in pure carbon fullerenes, a correlation between this energy and the observed fullerenes has been experimentally verified.[42] In fact, our low-energy atomic configurations shown in Figure 1a and b are characterized by having the largest highest occupied molecular orbital (HOMO)−lowest unoccupied molecular orbital (LUMO) energy separation, being of the order of ∼3.3 eV. Furthermore, for these particular atomic arrays, a well-defined closed electronic shell is also obtained, which are two well-known indicators of a high chemical stability in these kinds of carbon compounds. On the contrary, our less stable structures shown in Figure 1c−f are defined by reduced energy gaps ranging from 1.1 to 2.8 eV, and therefore, they are very likely to be reactive. Actually, our lowest energy configurations having large HOMO−LUMO energy gaps are expected to still stable be with increasing temperature, since, as has been demonstrated by Tozzini et al.,[43] the thermal stability of fullerene-like structures is strongly correlated with the width of this energy gap. Second, from the structural point of view, we have found that our lowest energy arrays shown in Figure 1a and b are characterized by the presence of a well-defined average C−O−H tilting angle of ∼108°. This is in qualitative agreement with the results obtained in extended surfaces where a high degree of molecular order is currently observed.

Concerning the role played by the hydrogen-bond formation between neighboring OH groups on the total energy of our carbon compounds, we have observed that it represents also a fundamental contribution. Actually, we have found that if we introduce a small or a large degree of orientational disorder in the hydroxyl layer shown in Figure 1a [by randomly changing the relative orientation of some (or all) of the adsorbed OH groups], we obtain variations in the total energy of the system as large as 6.8 eV. In particular, by perturbing the adsorbed (orientational) configuration of only five OH groups (located far away from each other on the surface) in the atomic structure shown in Figure 1a, we found that the fullerene compound becomes ∼5 eV less stable. On the other hand, if we consider now a fully disordered molecular OH layer, the atomic array is destabilized further by ∼6.8 eV. We can thus conclude by saying that the use of a theoretical methodology capable of describing the formation of hydrogen bonds on the C_{60} surface is necessary in order to correctly predict the structural properties of highly hydroxylated fullerenes.

It is clear that the different hydroxylations of the carbon surface shown in Figure 1 are expected to define different fullerenol compounds with contrasting physical and chemical properties. Furthermore, the properties of a particular isomer could be required for well-defined technological applications and of course it is important to ask if the different adsorbed phases shown in the figure have reached a state of organization that is spectroscopically distinguishable. In particular, the already discussed sizable modifications in the electronic spectra are expected to strongly perturb the optical response of each one of our considered isomers. Of course, the lowering in the degeneracies and the considerable HOMO−LUMO gap reopenings and closings modifies the number of energy levels and, in general, will change the spacing among them, a fact that could lead to different interband excitations and to sizable modifications in the location of the optical gap. As a consequence, theoretical calculations of the absorption spectra, that can be directly compared to the experimental measurements, could be very useful in order to try to identify the synthesized fullerene compounds.

In Figure 2, we show the calculated absorption spectra for some representative highly hydroxylated $C_{60}(OH)_{32}$ fullerenes. We consider contrasting configurations of adsorbed OH groups as the ones shown in Figure 1a, 1b, 1f, and 1g, and their corresponding distributions of electronic excitations are shown in parts a, b, c, and d of Figure 2, respectively. Note that in all cases we have restricted ourselves to the lowest lying electronic excited states, up to 4 eV (∼300 nm), for which the accuracy

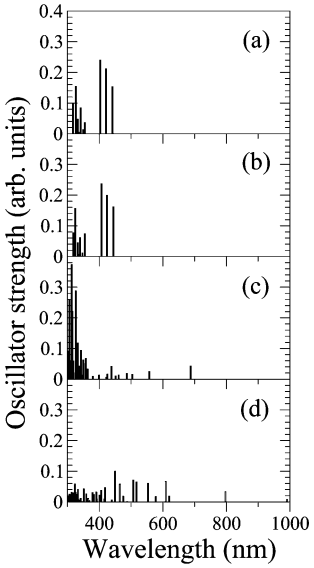

Figure 2. Calculated absorption spectra (excitation energy versus oscillator strength, in arbitrary units) for representative $C_{60}OH_{32}$ isomers using the ZINDO method. In parts a, b, c, and d, we show results for the configurations shown in parts a, b, f, and g of Figure 1, respectively. The vertical lines correspond to the calculated oscillator strength.

of the ZINDO methodology has been well established. From the figures, we note that the spectra of all of the hydroxylated fullerenes are very different from one another. Near the ultraviolet region, all low-symmetry molecules (see Figure 1) are characterized by broader absorption spectra having reduced intensities (see the region between 300 and 600 nm), when compared to the spectral distribution of the C_{60} fullerene which has only two dipole-allowed transitions located at 388 and 323 nm with oscillator strengths of 0.003 and 0.67, respectively. In addition, we notice from Figure 2 that, in the visible part of the spectra, the position and intensity of the electronic excitations also are very different. Our calculations reveal the existence of optical gaps located at wavelengths that vary in the range 421−991 nm (see Figure 2a and d as representative examples). At this point, it is important to mention that, despite the already discussed low stability of random configurations of OH groups on the C_{60} surface (see Figure 1g), molecules of this type are very interesting, since materials with their absorption expanded in the visible spectral region, that better matches the solar spectrum, are of crucial importance for the design of solar cell devices. Interestingly, we notice from Figure 2a and b that our low-energy structures (see Figure 1a and b) have almost identical absorption spectra, being characterized by two well-defined features, namely, (i) a complete absence of electronic excitations in the visible part of the spectra and (ii) the onset of optical excitations is located in the 420−440 nm range. Actually, we have found that when the size of the hydroxylated regions increases or the island formation is destroyed, the onset of the optical excitations shifts gradually to the visible part of the spectra. The previous spectral features together with our total energy calculations clearly provide a fingerprint to identify the presence of these types of fullerene derivatives.

At this point, it is important to mention that, as recently found by Husebo et al.[13] and Xing and co-workers,[14] in the case of fullerenols, the resulting reaction product seems to not always be simply polyhydroxylated C_{60}, as we have assumed in all of our previous calculations, but instead a complex fullerene compound containing also chemisorbed oxygen atoms that naturally appear in the reaction, and that it seems that they cannot be turned away from the formation process. As a

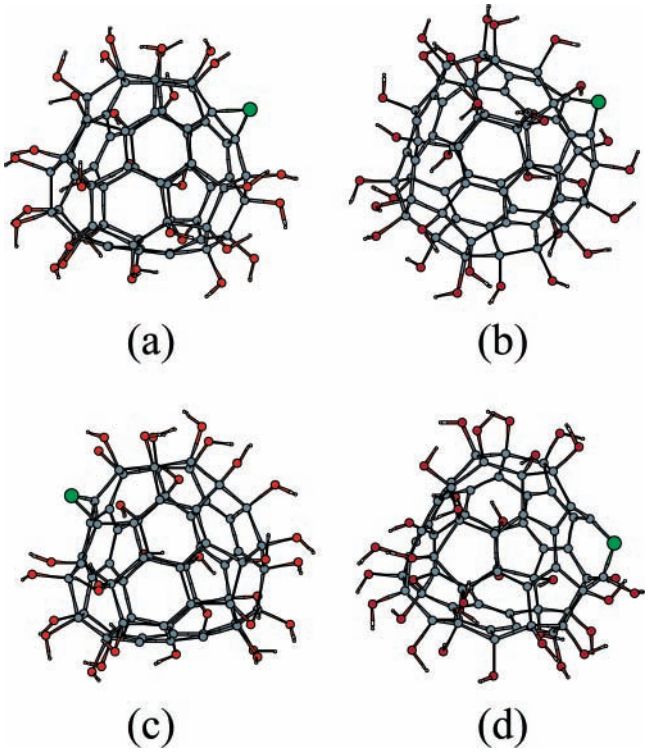

Figure 3. Optimized PM3 atomic configurations for representative $C_{60}OH_{32}O$ isomers. In part a, we show the lowest energy structure, and in parts b, c, and d, we show the three isomers that are closest in energy. The oxygen atom is denoted by a bigger filled circle.

consequence, we have performed additional calculations of the energetics and electronic behavior of fullerenol compounds but considering now a more heterogeneous composition in which we have included, besides the OH groups, up to four oxygen atoms in distinct positions on the carbon surface, namely, adsorbed within the highly hydroxylated parts of the cage (which slightly perturbs the optimal position of the OH groups shown in Figure 1a) as well as located in the unprotected regions of the surface, both close to the hydroxylated domains and also as isolated impurities in the uncovered parts of the C_{60}. For each number of adsorbed oxygens, we consider a total of 15 different initial configurations, and starting from our low-energy structure shown in Figure 1a, we allow, within the framework of the PM3 method, a full relaxation in response to oxygen incorporation on the surface. In a second step, these optimized configurations will be used as an input to perform, as in previous cases, single-point DFT calculations by using the B3LYP functional and the 6-21G basis set.

As a representative example, we show in Figure 3 some optimized structures for the $C_{60}(OH)_{32}$ fullerene shown in Figure 1a but containing a single oxygen impurity which, for the sake of clearness, is denoted by a bigger filled circle. In Figure 3a, we show the calculated lowest energy atomic configuration together with, in Figure 3b−d, the three closest in energy isomers. From the figures, we notice first that, as a consistent trend, the oxygen atom has been found to always be adsorbed over a C−C bond (on-bridge configuration) with C−O distances that vary in the range 1.37−1.42 Å. These structural parameters are in good agreement with the ones found in previous studies addressing the single oxygen adsorption on a bare C_{60} unit[44] as well as in pure carbon nanotubes.[45] Interestingly, we have found that the lowest energy structure corresponds to an atomic configuration (see Figure 3a) in which the oxygen atom prefers to be adsorbed in an uncovered part of the cage and not so close

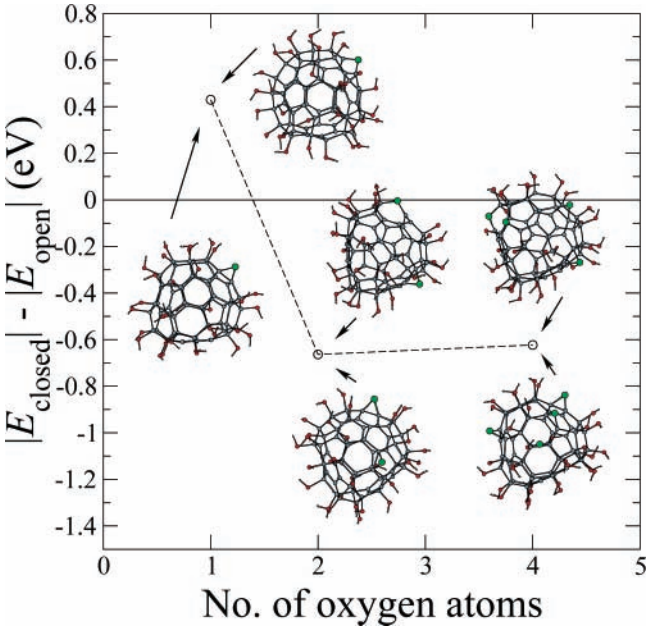

Figure 4. Calculated total energy difference (in eV) between closed- and open-cage configurations, $\Delta E = |E_{closed}| - |E_{open}|$ (with E defined as being negative), as a function of the number of adsorbed oxygen atoms. In the figure, we also show as insets the lowest energy atomic configurations for $C_{60}(OH)_{32}O$, $C_{60}(OH)_{32}O_2$, and $C_{60}(OH)_{32}O_4$ fullerenes.

to the hydroxylated regions. In addition, it is important to mention that the configuration in which the oxygen impurity is surrounded by the OH groups is not energetically preferred, a fact that suggests the existence of repulsive interactions between the coadsorbed O and OH species. This result, as will be seen in the following, will lead to the formation of well-defined domains of different chemical composition on the C_{60} surface.

From the point of view of theory, it is clear that, with an increasing number of oxygen atoms in our fullerenol compound shown in Figure 1a, a large amount of adsorbed configurations are possible. Consequently, our calculated lowest energy atomic arrays that will be presented in the following do not necessarily represent the absolute minimum; nevertheless, the resulting structures are probably representative examples of the interacting $C_{60} + OH + O$ system. Actually, it is important to remark that, as a consistent trend, we have always found that when both the coadsorbed oxygen and the OH group share the same carbon atom in the cage (as shown in Figure 3d) a bond breakage in the fullerene network is obtained in which a C−C bond is replaced by a carbon−oxygen−carbon bridge bond. The previous results clearly demonstrate that, on one hand, at least theoretically, it is always possible to obtain in a controlled way stable open-cage configurations and that, on the other hand, additional C−C bonds could also be broken if we increase the number of oxygen impurities on the surface.

As a consequence, to try to understand the observed experimental trend in ref 14, we plot now in Figure 4, for each one of the considered number of coadsorbed oxygen atoms, the calculated total energy difference between the lowest energy closed-cage configuration and the most stable open-cage atomic array, the latter being obtained using the procedure mentioned in the previous paragraph. Of course, it is clear that for one, two, and four oxygen impurities at least one, two, and four C−C bonds could be broken; however, as will be seen in the following, always the structures having only a single C−C broken bond on the surface will be the most stable arrays. From Figure 4, we notice that, for a single adsorbed oxygen, a closed-cage configuration corresponds to the most stable atomic array. However, for two and four chemisorbed O impurities, we have found that now highly hydroxylated fullerenes with a single broken C−C bond in the carbon network are instead preferred. Interestingly, the high stability of these fullerene compounds with broken C−C pairs is consistent with the recent experimental report of Xing et al.[14] who have found that the presence of oxygen atoms in fullerenols could lead to the formation of open-cage structures, a result that is of fundamental importance in several technological applications where the permanent encapsulation of a wide variety of atomic or molecular species in these types of fullerene derivatives is required. It seems thus that the energy gain obtained by the strain relief and the formation of a less repulsive environment overcomes the contribution to the cohesive energy due to the C−C bond formation, defining thus more stable carbon compounds.

In the lowest energy atomic configurations for the $C_{60}(OH)_{32}O_2$ fullerene included also as insets in Figure 4, we note that the two oxygen atoms are found to be adsorbed far away from each other and, as in the single impurity case, also over C−C bonds joining two neighboring hexagonal rings with C−O distances that are in the range ∼1.36−1.43 Å. At this point, it is important to remark that the large separation between the two O atoms is in contrast with the results obtained in the $C_{60}O_2$ compound where the two chemisorbed oxygens are adjacent to one another on a common six-membered ring.[46,47] In this respect, it is important to mention that, in our highly hydroxylated fullerenes, different bonding configurations for the oxygen species may develop, since the interaction between coadsorbed oxygens as well as between the O atoms and the carbon network could be altered by the effect of the neighboring OH molecules. However, in the case of the $C_{60}(OH)_{32}O_4$ compound, we have found that, in the lowest energy open-cage array, the four chemisorbed O atoms are located more close to each other in one side of the cage, a behavior that is consistent with the well-known aggregation of oxygen species when adsorbed on the bare C_{60} surface.[47,48] Interestingly, in our lowest energy open-cage $C_{60}(OH)_{32}O_x$ fullerenes shown in Figure 4, the C−O bond lengths range between 1.36 and 1.43 Å (indicating the existence of contrasting bonding environments), a distribution of distances that should be reflected in the vibrational spectra of the molecule, since a more broadened distribution of C−O vibrational modes is expected due to the different C−O bond lengths and different angles between the bonds connecting nearest-neighbor atoms.

It appears thus that in our considered fullerene compounds the energy is minimized when the fullerene surface consists of distinct highly hydroxylated and oxygenated regions and that OH-covered fullerenes exist as stable open-cage structures if small amounts of oxygen atoms are coadsorbed on the C_{60} surface, in good agreement with the experimental data of Xing et al.[14]

Finally, it is important to analyze also the electronic properties and the structural stability of fullerenols as multiply charged anions and cations. Both types of species can exist in gaseous[49] and aqueous[13,50] environments, and it is thus crucial to explore if our considered highly hydroxylated fullerenes remain stable relative to electron injection or detachment. In addition, it is important to mention that mass spectrometry experiments consider the difference in mass-to-charge ratio of ionized clusters to select them; therefore, one basic requirement for the detection of fullerenols is that they remain stable also when ionized. Consequently, we will analyze the structural stability of the low-energy $C_{60}(OH)_{32}$, $C_{60}(OH)_{32}O$, $C_{60}(OH)_{32}O_2$, and $C_{60}(OH)_{32}O_4$ fullerenes shown in Figures 1a and 4, respectively, as both

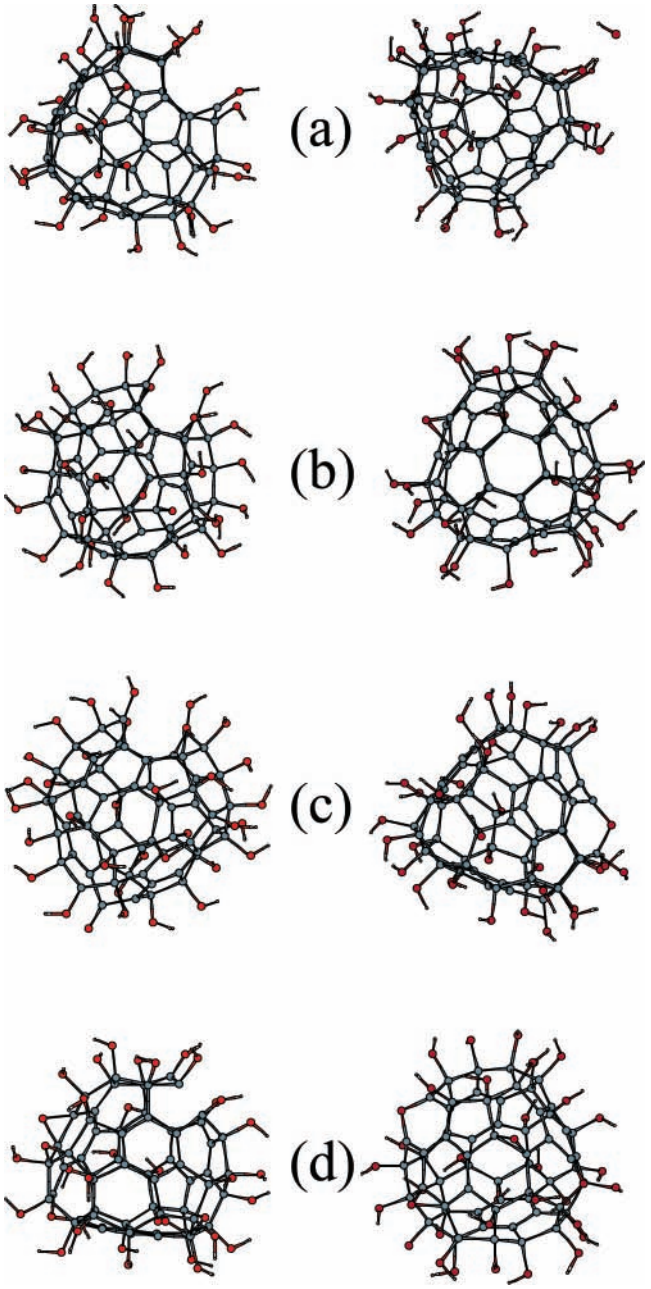

Figure 5. Optimized PM3 atomic configurations for cationic (left column) and anionic (right column) $C_{60}(OH)_{32}O_x^{\pm m}$ ($x = 0, 1, 2, 4$ and $m = 2, 4, 6$) species: (a) $C_{60}(OH)_{32}{}^{+6}$ (left) and $C_{60}(OH)_{32}{}^{-6}$ (right); (b) $C_{60}(OH)_{32}O^{+4}$ (left) and $C_{60}(OH)_{32}O^{-6}$ (right); (c) $C_{60}(OH)_{32}O_2{}^{+4}$ (left) and $C_{60}(OH)_{32}O_2{}^{-6}$ (right); (d) $C_{60}(OH)_{32}O_4{}^{+4}$ (left) and $C_{60}(OH)_{32}O_4{}^{-2}$ (right).

negatively and positively charged species. In Figure 5, we show our fully optimized $C_{60}(OH)_{32}O_x^{\pm m}$ compounds, where m will be as large as 6, which is a reasonable charge state that can be easily experimentally achieved. In the left (right) column, we plot our lowest energy atomic configurations obtained for fullerenol cations (anions). For the closed-cage configurations, we will continuously extract (add) an even number of electrons from (to) the structures until the first C−C broken bond is obtained. On the other hand, when considering carbon cages that are already partially open in the neutral state, we will add (extract) also an even number of electrons until an additional rupture of a C−C bond will be obtained. From the figure, we can distinguish contrasting structural features between both types of charged species. First, for the $C_{60}(OH)_{32}$ shown in Figure 5a, we note that, while in the positively charged structure (left) the detachment of six electrons is needed in order to obtain a C−C bond breakage that opens a sizable hole on the surface made of a 10-membered ring, in the fullerene anion (right), even with the inclusion of six electrons it was not possible to induce the rupture of the carbon structure. However, notice that, in this last case, a single OH group desorbs from the surface, a result that could imply that the fragmentation of the molecular coating could occur. Despite that, in both cases, significant structural rearrangements are obtained; the relatively high degree of ionization required to open the carbon cage clearly demonstrates, as already shown also in the previous paragraphs, the high stability of these kinds of adsorbed phases.

Interestingly, when our fullerenol compounds have a more complex composition consisting of coadsorbed oxygen atoms and OH groups, we have found that, in general, the opening of the cage structure can occur for a reduced charge state. This is clearly seen from Figure 5b where, even if in the open-cage $C_{60}(OH)_{32}O$ compound with six additional electrons (right) no C−C bonds are found to be broken, the positively charged $C_{60}(OH)_{32}O$ compound (Figure 5b, left) requires now the extraction of four electrons to attain the rupture of the carbon network in which a hole made of a 10-membered ring appears on the C_{60} surface. It is clear that this fullerene compound has a hole which is large enough to allow several types of guest molecules to enter or leave the cage.

In Figure 5c, we show the optimized geometries for cationic (left) and anionic (right) open-cage $C_{60}(OH)_{32}O_2$ species. Here, we have found that the extraction of four electrons is required to open an additional C−C bond in the carbon network (see Figure 5c, left) that opens a hole made of a nine-membered ring while, in the anionic array (see Figure 5c, right), even with the inclusion of six electrons it is not possible to obtain the rupture of additional C−C bonds. Interestingly, it is important to remark that, in our charged species, broken C−C pairs can be found not only just below the oxygen impurities but also in regions of the surface that are not so close to the location of the adsorbed O atoms. Of course, it is reasonable to expect that with increasing charge state in the molecules more complex structural rearrangements will occur, leading thus to the presence of bigger holes in the fullerene cavity. Finally, in Figure 5d, we show the lowest energy atomic configurations for the ionized $C_{60}(OH)_{32}O_4$ compound. In this case, we have found once again that the extraction of four electrons in the structure leads to the appearance of a hole made of a nine-membered ring while, in the negatively charged species, we note the existence of sizable surface reconstructions in which two C−C pairs containing an adsorbed oxygen are replaced by C−O−C bridge bonds, resulting also in the existence of a partially open carbon cage structure. Actually, in all of our open configurations, the C atoms forming the broken bonds are always highly charged with relatively large amounts of missing electrons, a result that considerably reduces their bonding strength and clearly leads to the rupture of the C−C pairs. From the previous results, we can thus conclude that the most possible structure of anionic and cationic oxygen-containing fullerenol species is in the form of open-cage configurations and that the gain or loss of electrons by ionization could be very useful for controlling the stability and the size of the opening of the cage in these kinds of highly hydroxylated compounds.

Finally, it is important to mention that our theoretical study has been dedicated to analyzing the electronic, optical, and structural properties of gas-phase-like $C_{60}(OH)_{32}O_x$ fullerenes. However, as is well-known, their synthetic routes as well as

the envisioned medical applications involved the presence of solvents, mainly water, and it is thus important to ask about the possible role of surrounding H_2O molecules on the here-reported theoretical data. In this respect, we believe that the formation of hydroxyl shells on the C_{60} as the ones shown in Figure 1 could act as efficient protective molecular layers. The surrounding water molecules are expected to be located close to the hydroxylated fullerene surface through the formation of hydrogen bonds, and as a consequence, both the electronic structure and relative stability will not be considerably perturbed due to the almost negligible H_2O-fullerenol charge transfer and the absence of new chemical bonds in the system. Of course, the previous expectations will not hold in low-hydroxylated fullerenes where the sizable amount of exposed carbon surface could lead to chemical reactions with the surrounding solvent molecules, leading thus to a sizable modification in the electronic and structural properties in the samples. Calculations are under way in order to corroborate the previous theoretical predictions.

IV. Summary and Conclusions

In this work, we have presented a systematic theoretical study, combining semiempirical and DFT approaches, of the structural, electronic, and optical properties of both neutral and ionized highly hydroxylated $C_{60}(OH)_{32}$ fullerenes. We have found that, in these highly OH-covered structures, lowest energy atomic configurations are obtained when the 32 OH groups are covering the C_{60} in the form of small and disconnected hydroxyl islands. Interestingly, these types of adsorbed phases seem to be a continuation of the growth sequence already found for the low-coverage regime in our previous work,[32] and their stability has been supported by well-defined electronic, structural, and total energy features. The calculated optical absorption spectra for different adsorbed phases have revealed that the value of the optical gap and, in general, the distribution of the electronic excitations are very sensitive to the location of the OH groups on the carbon surface, a fact that might provide an efficient way to identify the structure of these kinds of fullerene derivatives. Furthermore, in agreement with the experimental findings of Xing et al.,[14] we have found that oxygen-containing fullerenols exists as stable open-cage configurations.

Finally, the structural properties of both cationic and anionic fullerenol species reveal that a more dramatic cage destruction is obtained when charged hydroxylated C_{60} compounds are considered. In these cases, holes made of 9- and 10-membered rings can be present in the fullerene surface, through which a wide variety of atomic and molecular species might be able to enter or leave the cage. We believe that our results that have underlined the role played by the presence of coadsorbed oxygen impurities and the charge state of the cage are important if the controlled opening of carbon fullerenes is needed and should be taken into account also in several technological applications where the permanent encapsulation of several guest species in these types of carbon derivatives is required.

Acknowledgment. The authors would like to acknowledge the financial support from CONACyT (R.A.G.-L.) under project 45928-F and PROMEP (J.G.R.-Z.)

References and Notes

(1) Kroto, H. W.; Heath, J. R.; O'brien, S. C.; Curl, R. F.; Smalley, R. E. *Nature (London)* **1985**, *318*, 162.

(2) (a) Fanti, M.; Zerbetto, Z.; Galaup, J. P.; Rice, J.; Birkett, P.; Wachter, N.; Taylor, R. *J. Chem. Phys.* **2002**, *116*, 7621. (b) Coheur, P. F.; Cornil, J.; dos Santos, D. A.; Birkett, P.; Lievin, J.; Bredas, J. L.; Walton, D. R. M.; Taylor, R.; Kroto, H. W.; Colin, R. *J. Chem. Phys.* **2000**, *112*, 6371. (c) Riggs, J. E.; Sun, Y. P. *J. Chem. Phys.* **2000**, *112*, 4221.

(3) (a) Coheur, P. F.; Cornil, J.; dos Santos, D. A.; Birkett, P.; Lievin, J.; Bredas, J. L.; Walton, D. R. M.; Taylor, R.; Kroto, H. W.; Colin, R. *J. Chem. Phys.* **2000**, *112*, 8555. (b) Coheur, P. F.; Lievin, J.; Colin, R.; Razbirib, B. *J. Chem. Phys.* **2003**, *118*, 550. (c) Xie, R. H.; Bryant, G. W.; Cheung, C. F.; Smith, V. H.; Zhao, J. *J. Chem. Phys.* **2004**, *121*, 2849.

(4) (a) Sitharaman, B.; Bolskar, R. D.; Rusakova, I.; Wilson, L. J. *Nano Lett.* **2004**, *4*, 2373. (b) Sayes, C. M.; Fortner, J. D.; Guo, W.; Lyon, D.; Boyd, A. M.; Ausman, K. D.; Tao, Y. J.; Sitharaman, B.; Wilson, L. J.; Hughes, J. B.; West, J. L.; Colvin, V. L. *Nano Lett.* **2004**, *4*, 1881. (c) Toth, E.; Bolskar, R. D.; Borel, A.; Gonzalez, G.; Helm, L.; Merbach, A. E.; Sitharaman, B.; Wilson, L. J. *J. Am. Chem. Soc.* **2005**, *127*, 799.

(5) Rincón, M. E.; Hu, H.; Campos, J.; Ruiz-García, J. *J. Phys. Chem. B* **2003**, *107*, 4111.

(6) (a) Friedman, S. H.; DeCamp, D. L.; Sijbesma, R. P.; Srdanov, G.; Wudl, F.; Kenyon, G. L. *J. Am. Chem. Soc.* **1993**, *115*, 6506. (b) Marcorin, G. L.; Ros, T. D.; Castellano, S.; Stefancich, G.; Bonin, I.; Miertus, S.; Prato, M. *Org. Lett.* **2000**, *2*, 3955.

(7) Tokuyama, H.; Yamago, S.; Nakamura, E.; Shiraki, T.; Sugiura, Y. *J. Am. Chem. Soc.* **1993**, *115*, 7918.

(8) Schinazi, R. F.; Sijbesma, R.; Srdanov, G.; Hill, C. L.; Wudl, F. *Antimicrob. Agents Chemother.* **1993**, *37*, 1707.

(9) Dugan, L. L.; Turetsky, D. M.; Du, C.; Lobner, D.; Wheeler, M.; Almli, C. R.; Shen, C. K. F.; Lu, T. Y.; Choi, D. W.; Lin, T. S. *Proc. Natl. Acad. Sci. U.S.A.* **1997**, *94*, 9434.

(10) Krusic, P. J.; Keiser, J.; Morton, J. R.; Preston, K. F. *Science* **1991**, *254*, 1183.

(11) (a) Mikawa, M.; Kato, H.; Okumure, M.; Narazaki, M.; Kanazawa, Y.; Miwa, N.; Shinohara, H. *Bioconjugate Chem.* **2001**, *12*, 510. (b) Tóth, E.; Bolskar, R. D.; Borel, A.; González, G.; Helm, L.; Merbach, A. E.; Sitharaman, B.; WIlson, L. J. *J. Am. Chem. Soc.* **2005**, *127*, 799.

(12) Chiang, L. Y.; Upasani, R. B.; Swirczewsky, J. W. *J. Am. Chem. Soc.* **1992**, *114*, 10154.

(13) Husebo, L. O.; Sitharaman, B.; Furukawa, K.; Kato, T.; Wilson, L. J. *J. Am. Chem. Soc.* **2004**, *126*, 12055.

(14) Xing, G.; Zhang, J.; Zhao, Y.; Tang, J.; Zhang, B.; Gao, X.; Yuan, H.; Qu, L.; Cao, W.; Chai, Z.; Ibrahim, K.; Su, R. *J. Phys. Chem. B* **2005**, *108*, 11473.

(15) Sitharaman, B.; Asokan, S.; Rusakova, I.; Wong, M. S.; Wilson, L. J. *Nano Lett.* **2004**, *4*, 1759.

(16) (a) Murata, Y.; Murata, M.; Komatsu, K. *J. Am. Chem. Soc.* **2003**, *125*, 7152. (b) Komatsu, K.; Murata, M.; Murata, Y. *Science* **1995**, *307*, 238.

(17) Shinohara, H. *Rep. Prog. Phys.* **2000**, *63*, 843.

(18) Saunders, M.; Cross, R. J.; Jiménez-Vázquez, H. A.; Shimshi, R.; Khong, A. *Science* **1996**, *271*, 1693.

(19) Khaled, M. M.; Carlin, R. T.; Trulove, P. C.; Eaton, G. R.; Eaton, S. S. *J. Am. Chem. Soc.* **1994**, *116*, 3465.

(20) Stewart, J. J. P. *J. Comput. Chem.* **1989**, *10*, 209.

(21) (a) Becke, A. *Phys. Rev. A* **1988**, *38*, 3098. (b) Lee, C.; Yang, W.; Parr, R. G. *Phys. Rev. B* **1988**, *36*, 785.

(22) Binkley, J. S.; Pople, J. A.; Henre, W. J. *J. Am. Chem. Soc.* **1980**, *102*, 939.

(23) Zerner, M. C. In *Reviews in Computational Chemistry II*; Lipkowitz, K. B., Boyd, D. B., Eds.; VCH: Weinheim, Germany, 1991; Chapter 8, pp 313−336.

(24) Frisch, M. J.; Trucks, G. W.; Schlegel, H. B.; Scuseria, G. E.; Robb, M. A.; Cheeseman, J. R.; Zakrzewski, V. G.; Montgomery, J. A., Jr.; Stratmann, R. E.; Burant, J. C.; Dapprich, S.; Millam, J. M.; Daniels, A. D.; Kudin, K. N.; Strain, M. C.; Farkas, O.; Tomasi, J.; Barone, V.; Cossi, M.; Cammi, R.; Mennucci, B.; Pomelli, C.; Adamo, C.; Clifford, S.; Ochterski, J.; Petersson, G. A.; Ayala, P. Y.; Cui, Q.; Morokuma, K.; Malick, D. K.; Rabuck, A. D.; Raghavachari, K.; Foresman, J. B.; Cioslowski, J.; Ortiz, J. V.; Baboul, A. G.; Stefanov, B. B.; Liu, G.; Liashenko, A.; Piskorz, P.; Komaromi, I.; Gomperts, R.; Martin, R. L.; Fox, D. J.; Keith, T.; Al-Laham, M. A.; Peng, C. Y.; Nanayakkara, A.; Challacombe, M.; Gill, P. M. W.; Johnson, B.; Chen, W.; Wong, M. W.; Andres, J. L.; Gonzalez, C.; Head-Gordon, M.; Replogle, E. S.; Pople, J. A. *Gaussian 98*, revision A.9; Gaussian, Inc.: Pittsburgh, PA, 1998.

(25) Hedberg, K.; Hedberg, L.; Bethune, D. S.; Brown, C. A.; Dorn, H. C.; Johnson, R. D.; de Vries, M. *Science* **1991**, *254*, 410.

(26) Haser, M.; Almlof, J.; Scuseria, G. E. *Chem. Phys. Lett.* **1991**, *181*, 497.

(27) (a) Gasyna, Z.; Schatz, P. N.; Hare, J. P.; Denis, T. J.; Kroto, H. W.; Taylor, R.; Walton, D. R. M. *Chem. Phys. Lett.* **1991**, *183*, 283. (b) Coheur, P. F.; Carleer, M.; Colin, R. *J. Phys. B* **1996**, *29*, 4897.

(28) (a) Hora, J.; Panek, P.; Navratil, K.; Handlirova, B.; Humlicek, J. *Phys. Rev. B* **1996**, *54*, 5106. (b) Fujitzuka, M.; Ito, O.; Maeda, Y.; Kako, M.; Wakahara, T.; Akasaka, T. *Phys. Chem. Chem. Phys.* **1999**, *1*, 3527.

(29) Xie, R. H.; Bryant, G. W.; Sun, G.; Nicklaus, M. C.; Heringer, D.; Frauenheim, T.; Manaa, M. R.; Smith, V. H.; Araki, Y.; Ito, O. *J. Chem. Phys.* **2004**, *120*, 5133.

(30) Meier, M. S.; Kiegiel, J. *Org. Lett.* **2001**, *3*, 1717.

(31) Pan, H.; Feng, Y. P.; Lin, J. Y. *Phys. Rev. B* **2004**, *70*, 245425.

(32) Rodríguez-Zavala, J. G.; Guirado-López, R. A. *Phys. Rev. B* **2004**, *69*, 075411.
(33) Bedürftig, K.; Völkening, S.; Wang, Y.; Wintterlin, J.; Jacobi, K.; Ertl, G. *J. Chem. Phys.* **1999**, *111*, 11147.
(34) Fowler, P. W.; Collins, D. J.; Austin, S. J. *J. Chem. Soc., Perkin Trans.* **1993**, *2*, 275.
(35) Birkett, P. R.; Avent, A. G.; Darwish, A. D.; Kroto, H. W.; Taylor, R.; Walton, D. R. M. *J. Chem. Soc., Chem. Commun.* **1993**, 1230.
(36) Slanina, Z.; Zhao, X.; Chiang, L. Y.; Osawa, E. *Int. J. Quantum Chem.* **1999**, *74*, 343.
(37) Wang, B.-C.; Cheng, C.-Y. *THEOCHEM* **1997**, *391*, 179.
(38) Palpant, B.; Negishi, Y.; Sanekata, M.; Miyajima, K.; Nagao, S.; Judai, K.; Rayner, D. M.; Simard, B.; Hackett, P. A.; Nakajima, A.; Kaya, K. *J. Chem. Phys.* **2001**, *114*, 8495.
(39) Dugourd, Ph.; Antoine, R.; Rayane, D.; Compagnon, I.; Broyer, M. *J. Chem. Phys.* **2001**, *114*, 1970.
(40) Roques, J.; Calvo, F.; Spiegelman, F.; Mijoule, C. *Phys. Rev. Lett.* **2003**, *90*, 075505.
(41) Sun, Q.; Wang, Q.; Jena, P.; Kawazoe, Y. *J. Am. Chem. Soc.* **2005**, *127*, 14582.
(42) Kietzman, H.; Rochow, R.; Ganteför, G.; Eberhardt, W.; Vietze, K.; Seifert, G.; Fowler, P. W. *Phys. Rev. Lett.* **1998**, *81*, 5378.
(43) Tozzini, V.; Buda, F.; Fasolino, A. *Phys. Rev. Lett.* **2000**, *85*, 4554.
(44) (a) Menon, M.; Subbaswamy, K. R. *Phys. Rev. Lett.* **1991**, *67*, 3487. (b) Weisman, R. B.; Heymann, D.; Bachilo, S. M. *J. Am. Chem. Soc.* **2001**, *123*, 9720. (c) Xu, X.; Shang, Z.; Wang, G.; Cai, Z.; Pan, Y.; Zhao, X. *J. Phys. Chem. A* **2002**, *106*, 9284.
(45) (a) Foudrakis, G. E.; Schnell, M.; Mühlhaüser, M.; Peyerimhoff, S. D.; Andriotis, A. N.; Menon, M.; Sheetz, R. M. *Phys. Rev. B* **2003**, *68*, 115435. Dag, S.; Gülseren, O.; Yildirim, T.; Ciraci, S. *Phys. Rev. B* **2003**, *67*, 165424.
(46) Balch, A. L.; Costa, D. A.; Noll, B. C.; Olmstead, M. M. *J. Am. Chem. Soc.* **1995**, *117*, 8926.
(47) Fusco, C.; Seraglia, R.; Curci, R.; Lucchini, V. *J. Org. Chem.* **1999**, *64*, 8363.
(48) Tajima, Y.; Takeuchi, K. *J. Org. Chem.* **2002**, *67*, 1696.
(49) (a) Sookhun, S.; Dunn, J. L.; Bates, C. A. *Phys. Rev. B* **2003**, *68*, 235403. (b) Dunn, J. L.; Li, H. *Phys. Rev. B* **2005**, *71*, 115411. (c) Cammarata, V.; Guo, T.; Illies, A.; Li, L.; Shevlin, P. *J. Phys. Chem. A* **2005**, *109*, 2765. (d) Díaz-Tendero, S.; Alcamí, M.; Martín, F. *Phys. Rev. Lett.* **2005**, *95*, 013401.
(50) Dubois, D.; Kadish, K. M.; Flanagan, S.; Wilson, L. J. *J. Am. Chem. Soc.* **1991**, *113*, 7773.